SSCL-637

SSCL-637
August 1993
Distribution Category: 40

V. Kovachev
M. Neal
J. Seuntjens
J. Madison
S. Graham
P. Cline
M. Wake
D. Capone II

Interstrand Resistance of DSA328 Coil

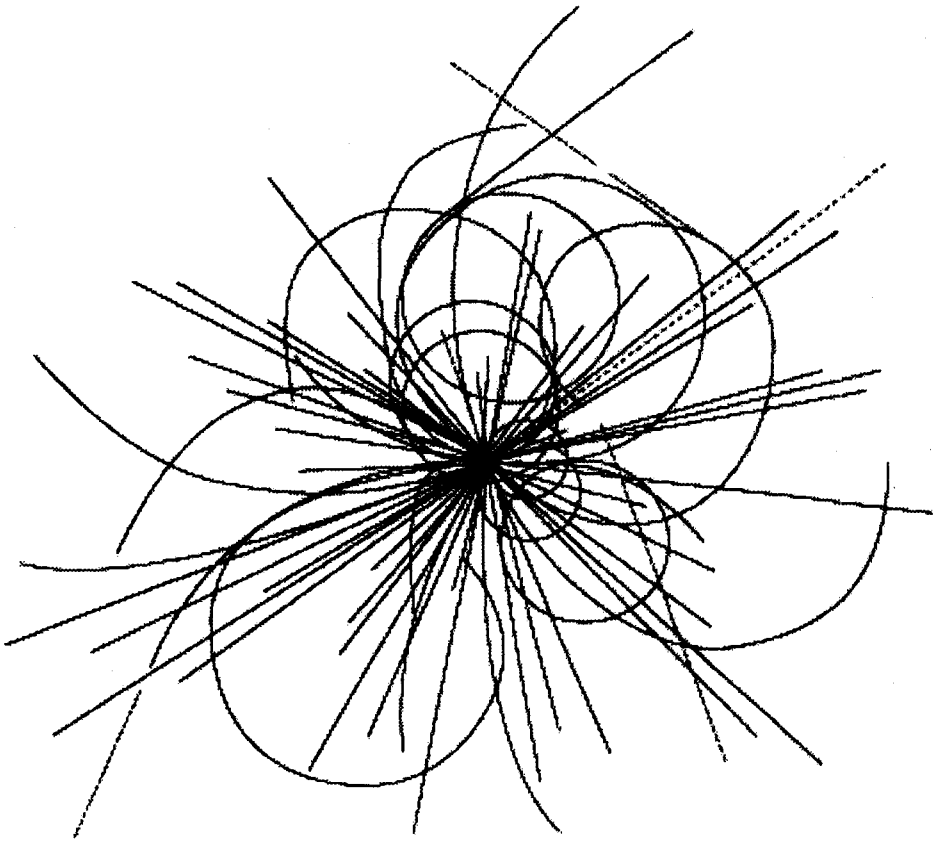

Superconducting Super Collider Laboratory

SSCL-637

Interstrand Resistance of DSA328 Inner Coil

V. Kovachev, M. Neal, J. Seuntjens, J. Madison,
S. Graham, P. Cline, and D. Capone II

Superconducting Super Collider Laboratory*
2550 Beckleymeade Ave.
Dallas, TX 75237

M. Wake†

National Laboratory for High Energy Physics
1-1 Oho, Tsukuba, Ibaraki, 305 Japan

August 1993

*Operated by the Universities Research Association, Inc., for the U.S. Department of Energy under Contract No. DE-AC35-89ER40486.

†On leave from National Laboratory for High Energy Physics, 1-1 Oho, Tsukuba, Ibaraki, 305 Japan.

1.0 INTRODUCTION

The performance of full length SSC dipole magnets has demonstrated that 50 mm aperature dipoles are much more sensitive to the current ramp rate than their predecessors with 40 mm aperture.[1] Moreover, the magnet quench current (I_q) at high ramp rates exhibits a very large magnet-to-magnet spread. There are two quite distinct families of curves for the quench current vs. the current (field) ramp rate of full length dipole magnets. The first one (type A) shows an initial nearly flat quench current up to about 20 A/s, then an almost linear decrease of the quench current with the ramp rate. The linear portion slope of the $I_q(dI/dt)$ curve, however, varies largely among the magnets of this family. The second family of magnets (type B) shows a rapid initial decrease in quench current at low ramp rates followed by an almost constant quench current at high ramp rates. The 50 mm short model dipoles basically have shown similar behavior but somewhat less pronounced.[2] Also, there are some short magnets as well as full length magnets which do not show either type A or type B quench behavior.

Energy loss during field ramp of type A and type B magnets are also different. Type A magnets exhibit very large eddy current losses at high ramp rates. Type B dipoles have a relatively small eddy current loss during the ramp. The eddy current loss in magnets has two components: intrastrand loss and interstrand loss. Different coil curing procedures may lead to some differences in strand RRR recovery and consequently to some differences in intrastrand eddy current coupling. This alone, however, cannot explain the magnet test results showing large differences in eddy current dissipation for type A and type B magnets. Obviously, for some reason, eddy currents between strands vary considerably among magnets resulting in a difference observed in the total amount of eddy current loss. The major contribution to interstrand energy loss comes from the magnet inner coil because of the higher field derivative. There is direct experimental evidence that quenches in A type magnets are related to this extra eddy current energy release. When such a magnet is excited slowly (for instance with a ramp rate of about 10 A/s) the quench locations are at the magnet pole because the field intensity at the pole is the highest. When the ramp rate increases the quench current goes down and the quench location moves to the multi-turn section of the inner coil where the magnetic field is perpendicular to the wide face of the cable and large interstrand eddy currents result. This is also the region of the inner coil where heat removal is most difficult. Large eddy current loss and quench location movement to the multi-turn section in type A magnets suggest the existence of relatively low interstrand resistance in the bulk of magnet inner coils.

For type B magnets the interpretation of quench sensitivity is not so simple. However, it is believed that very low interstrand resistance between a single pair of strands together with generally high interstrand resistance for the rest of the strands can be the source for type B quench of magnets. The low interstrand resistance will allow considerable eddy current to be induced and added to the transport current of certain strands which may be brought up to quench. Large local eddy currents may also cause local overheating but because of the good thermal conductivity of the cable it should be a second order effect for the early quench. On the other hand, difficult current and heat sharing between the strands due to large interstrand resistance can also contribute to magnets quenching in a B type manner.

The above stated correlations show how important it is to study the interstrand resistance in real magnet coils in order to help solve the quench current sensitivity problem for HEB dipole magnets. The knowledge of interstrand resistance distribution across the magnet coil is also important for CDM in terms of multipole decay.

The aim of the present work is to obtain accurate data for interstrand resistance and interstrand resistance distribution in a section of DSA328 (FNAL built SSC short model magnet) using an *in situ* method. *In situ* measurements of interstrand resistance in accelerator magnets have never been reported in the literature. The present work is the first attempt to describe this method and to discuss obtained results.

2.0 EXPERIMENTAL METHOD

2.1 History of Magnet DSA 328

The electromagnetic design of magnet DSA328 was done at BNL. The mechanical design, assembly and the test of this magnet was performed at FNAL.

The quench current vs the ramp rate for DSA328 is shown on Figure 1. The quench current behavior is somewhat in between A and B type — almost a flat quench current up to about 50 A/s and type B like decrease (but more rapid than usual) of the quench current with the ramp rate up to 300 A/s. The first quenches (at dI/dt < 20 A/s) have occurred at the inner pole turn splice side. At dI/dt > 20 A/s the quenches have moved to the non pole turn section of the inner coil, *i.e.* ,where the magnetic field has a larger angle with the wide face of the cable.

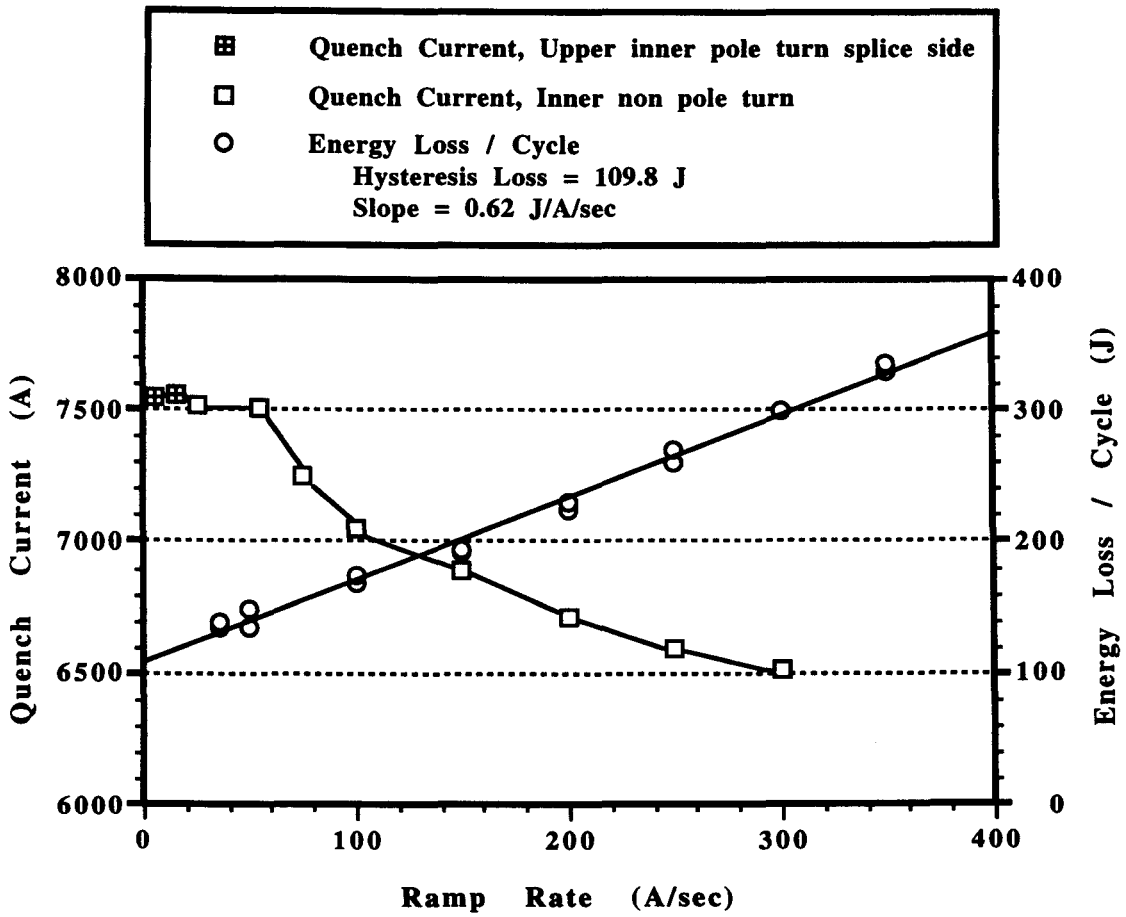

Figure 1. Quench Current and AC Losses as a Function of Current Ramp Rate for Magnet DSA 328.

The AC losses vs. the ramp rate for magnet DSA328 are also shown in Figure 1. The energy loss per cycle is a linear function of the ramp rate. The slope of this line represents the eddy current portion of the loss. For DSA328 this slope is 0.62 J/(A/s) which represents moderate eddy current loss for SSC 50 mm short model magnets. Eddy current losses do not vary much for these magnets, for instance the magnet DSA324 has eddy current loss of 0.66 J/A/s and the magnet DSA323 has eddy current dissipation of 0.58 J/(A/s).

2.2 Preparation of Magnet Section

A section of the magnet DSA328 15.4 cm in length was prepared for *in situ* interstrand resistance measurements. The yoke of this section was removed but the collar and the collar pressure was left on the coil section. All four keys are spot-welded every 2–3 cm in a zig-zag manner on both key sides. The keys were cut and removed 4 cm from one end of the section (end A). The outer coil is also removed 4 cm from end A. Both ends of the inner coil (A and B) were machined using a lathe. The end B was then polished and etched to avoid short circuits between superconducting filaments from adjacent strands or turns. Thus the final test configuration consists of a collared coil section 11.4 cm in length and exposed 4 cm long portions of the inner coils. The collared section is slightly longer than the cable pitch length (86 mm) so that there are at least two contacts for any combination of wires within a cable. The exposed portions of the inner coils were designed to allow easy access for electrical connection to the test equipment. Figure 2 is a sketch of the magnet section showing the exposed turns of the inner coils.

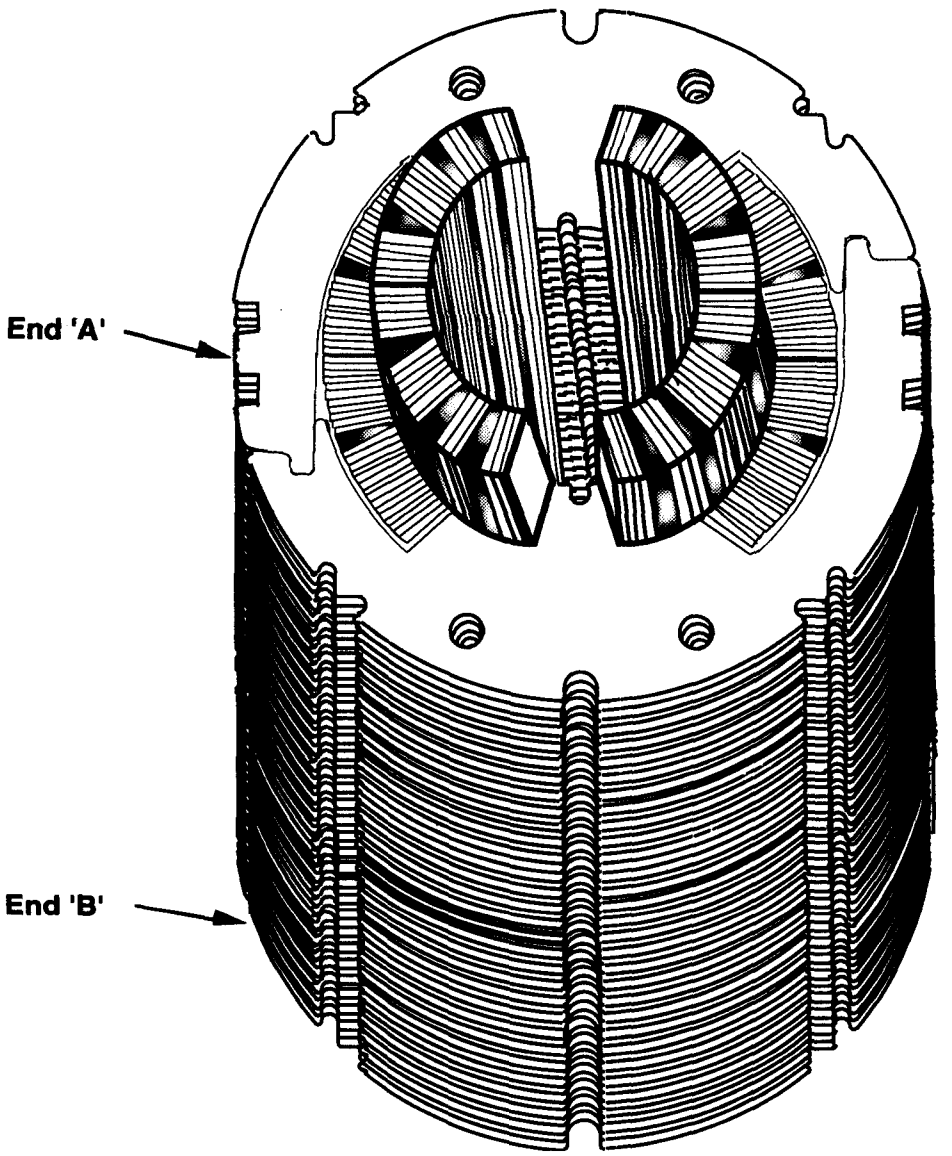

Figure 2. Sketch of the Magnet Segment, Showing the Exposed Turns of the Inner Coils.

2.3 Test Procedure

The *in situ* interstrand resistance measurements were performed using the standard four-probe technique. The current leads were made of teflon insulated 10 gauge copper wire. The bottom portion of the current leads consists of 15–20 cm of NbTi multifilamentary wire (SSC inner strand) to allow easy connection to the test section and to reduce the heat to the LHe bath. The voltage taps were made of varnish insulated 30 gauge copper wire. The sample holder contains 12 current leads and 12 twisted voltage tap leads. The sample holder consists simply of two flanges made of G-10 fiberglass (250 mm and 140 mm in diameter) and a G-10 rod (16 mm in diameter) connecting these two flanges. The coil section is situated on the 140 mm flange and instrumented with current and voltage tap leads. The upper flange serves as a top plate for the cryostat. Prior to cooling down to 4.2 K the magnet section was precooled to LN temperature then inserted into the helium cryostat. A simple LHe dewar with superinsulation and large aperture was used as the 4.2 K cryostat.

The turns of the inner coils were labeled in the conventional manner from 1 (midplane turn) to 19 (pole turn) as shown in the sketch in Figure 3.

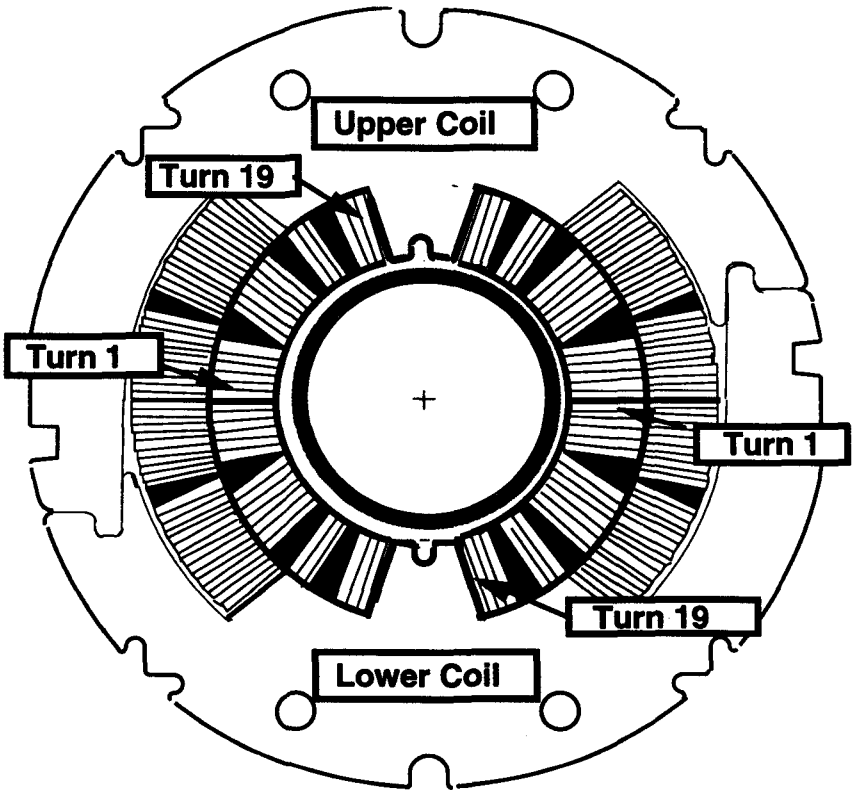

Figure 3. Sketch of the Cross Section of Magnet DSA 328.

In one cooldown the inner coil turns were tested for interstrand resistance in pairs, one turn from each of the two coils, which were arbitrarily labeled the upper and lower coils. As each measurement of one turn in a coil was completed the strand ends of that turn were cut away to reveal the strand ends of the next turn. In this way 19 turns (from the pole turn to the midplane) of both coils in the magnet were measured in succession. The cable strands at a given test point were labeled from 1 to 30 counterclockwise from the inside minor edge as shown in Figure 4. Sets of six of these strands were prepared for interstrand resistance testing. A set consisting of equally spaced non-adjacent strands (1, 6, 11, 16, 21, and 26) was tested for each turn of both magnet coils.

In addition a set of six adjacent strands (1–6) was tested for turns 1–5 of both coils and turn 19 of the upper coil. The six strands in each set were paired for testing in all possible combinations, generating a total of 15 resistance measurements. The measurements were carried out at 4.2 K using the standard four probe technique, in which a sample current of from 10–50 amperes was used and a voltage drop on the order of 20 μV across the two strands was recorded. The typical thermal voltage was not greater than 1 μV. The reproducibility of the results was better than 5% even in the case of separate cooldowns. The current was supplied by a Hewlett Packard 6031A System Power Supply and the voltage was recorded using a Keithley 182Sensitive Digital Voltmeter. Output from the power supply was passed through the center of a zero flux transformer, inducing a proportional voltage in the transformer which was monitored by another Keithley 182 Voltmeter. Figure 4 is a schematic of the magnet cable which identifies the groups of strands tested in this way.

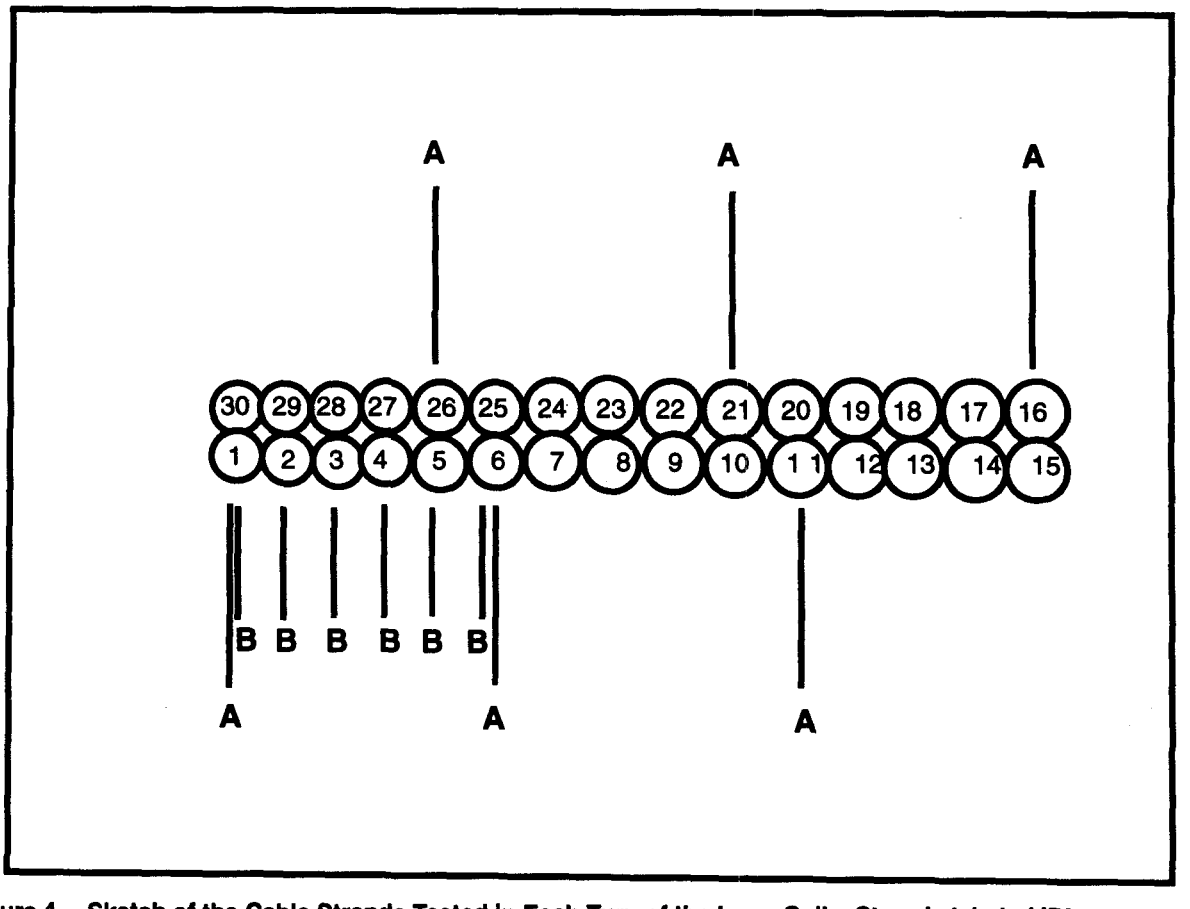

Figure 4. Sketch of the Cable Strands Tested in Each Turn of the Inner Coils. Strands labeled 'B' were used to measure adjacent strand resistance, 'A' strands were used to test nonadjacent strand resistance.

3.0 RESULTS AND DISCUSSION

The entire set of data for the interstrand resistance of the DSA328 inner coil is presented in Appendix I. This set contains approximately 750 interstrand resistance values for the inner upper and the inner lower coil of DSA328. The average interstrand resistance numbers for each turn are shown in Table 1.

The first column of Table 1 shows the average resistance between non-adjacent strands which is the average of 15 measurements (see Figure 4): (1)–(6), (1)–(11), (1)–(16), (1)–(21), (1)–(26), (6)–(11),

(6)–(16), (6)–(21), (6)–(26), (11)–(16), (11)–(21), (11)–(26), (16)–(21), (16)–(26), (21)–(26). The second column of Table 1 presents the average resistance for adjacent strands which is an average of 5 measurements: (1)–(2), (2)–(3), (3)–(4), (4)–(5), (5)–(6). The adjacent strand resistance average is considerably lower than the average resistance between non-adjacent strands. This is to be expected due to the different nature of adjacent and nonadjacent contacts. In addition to the relatively large surface area of adjacent strand side-by-side contact, the strands transpose at the edge of the cable so that they roll over one another. This rollover takes place over quite a long distance along the cable axis and involves more strand deformation than non-adjacent strand crossover. At the cable edges the compaction of the cable is largest. The experimental technique used for interstrand resistance measurements can not distinguish between side-by-side and rollover contacts. In reality a combination of both can cause low interstrand resistance between adjacent strands.

TABLE 1. AVERAGE INTERSTRAND RESISTANCE VALUES FOR ADJACENT AND NONADJACENT STRAND PAIRS IN MAGNET DSA 328.

	UPPER COIL		LOWER COIL	
TURN #	NON-ADJACENT	ADJACENT	NON-ADJACENT	ADJACENT
19 (pole)	11.7 μΩ	3.0 μΩ	5.0 μΩ	3.0 μΩ
18	5.8	1.4	3.3	1.3
17	0.8	0.2	2.4	1.1
Cu Wedge				
16	1.9	0.3	3.2	1.8
15	1	0.2	1.5	0.4
14	0.8		2.4	
Cu Wedge				
13	1.2		2.7	
12	1		1.7	
11	2.8		2.8	
10	0.9		2.3	
9	0.9		2.5	
8	2.4		1.7	
7	3.4		2.0	
Cu Wedge				
6	7		2.3	
5	2.1		1.1	
4	2.6		1.3	
3	2.8		1.3	
2	2.8		1.4	
1 (midplane)	2.2		1.4	

Relatively low adjacent strand interstrand resistance can influence the interstrand resistance measured for non-adjacent strand. The interplay between adjacent strand major contacts (rollover and/or side by side) and non-adjacent strands major contacts (crossover) will be explained below by means of a simple model.

The measured interstrand resistance as a function of strand separation for a given turn of the magnet generally shows a second order polynomial type of curve which in some cases appears as a simple parabola. These simple parabolas were more common for the upper (arbitrary chosen as upper) coil data. Figure 5 shows data from turn 16 of the upper coil which has this parabolic shape and turn 19 of the lower coil which has the more general second order polynomial shape. As will be discussed below, in both cases predominate conductance between all strands must be identical otherwise the experimental data will not lie on the typical curves.

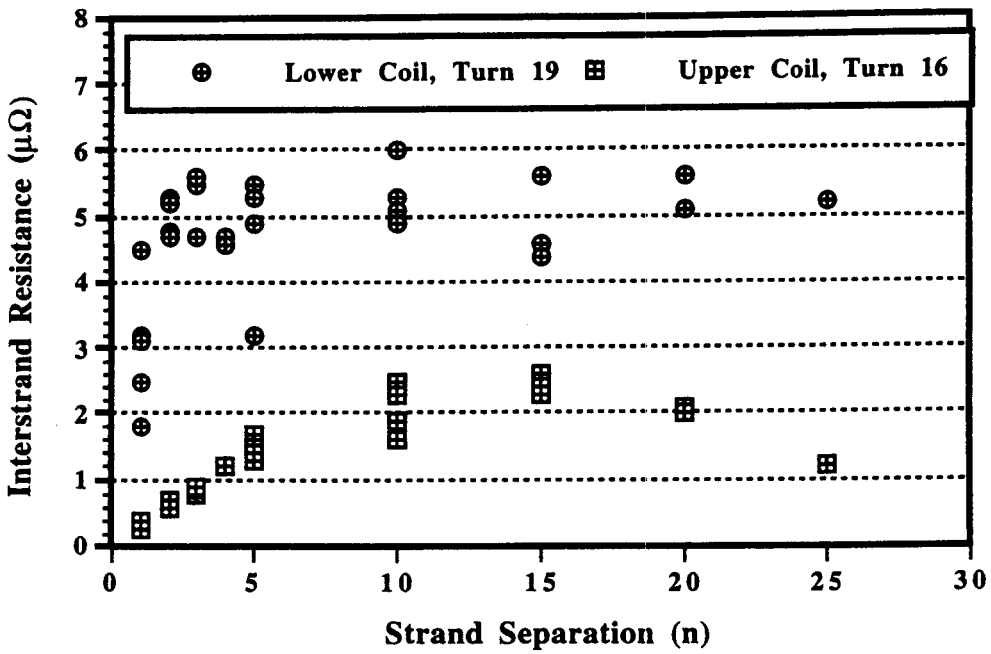

Figure 5. Interstrand Resistance as a Function of Strand Separation for Turn 16 of the Upper Coil and Turn 19 of the Lower Coil.

The simple model for evaluation of the contact resistance considers two limiting cases. In the first case rollover/side-by-side contacts are neglected. Every combination of strands makes 2 primary contacts for one cable pitch length. All crossover contacts are assumed equal. All crossover paths beyond the secondary ones are neglected. The equivalent circuit and final formula deduction for this case is given in Appendix II. A single measured crossover resistance is given by:

$$R_{co} = r_{co}/N \tag{1}$$

where r_{co} is the crossover resistance value, and N is the number of strands in the cable.

In the second case the crossover contacts between strands are neglected. The equivalent circuit and final formula deduction for this case is also given in Appendix II. A single rollover/side by resistance is given by:

$$R_{adj} = \frac{r_{adj}}{N}\left[N^2/4 - \left(n - \frac{N}{2}\right)^2\right] \tag{2}$$

where r_{adj} is the rollover/side by side resistance, N is as before, and n is the difference between strand numbers shown in Figure 4.

In reality in many cases both the crossover and the rollover/side by side contacts can not be neglected and the measured resistance (see appendix II) is given by:

$$R_{tot} = r_{co}r_{adj}n(N - n)/N\left(r_{co} + r_{adj}n(N - n)\right) \tag{3}$$

where r_{co}, r_{adj}, N, and n are as above. Equation 3 can be manipulated algebraically to form Equation 4, which is a linear equation in 1/R and $(N/(Nn-n^2))$.

$$\frac{1}{R_{tot}} = \frac{1}{r_{co}}\left(N/\left(Nn - n^2\right)\right) + \frac{N}{r_{adj}} \tag{4}$$

It is clear from Equation 4 that a plot of measured interstrand conductance (1/R) as a function of the strand separation parameter ($N/(Nn-n^2)$ will be a straight line, the slope of which is the adjacent (side-by-side/rollover) interstrand conductance, and the y-axis intercept is the product of N, the total number of strands in the cable, and the nonadjacent (crossover) interstrand conductance. Central to this analysis are the assumptions that all side-by-side/rollover resistances and all crossover resistances are identical. The extent to which this assumption is not valid will be reflected in the deviation of the data from linearity. Figure 6 shows interstrand resistance data from turns 1 and 15 of the upper coil plotted in the coordinate system of Equation 4. Adjacent strand data is plotted at the extreme right in this graph, and the apparent spread in this data is due to the low resistance values measured and the fact that the data is plotted as a conductance. For example, the data presented for turn 15, n=1 ranges only from 0.18 to 0.26 μΩ, and for n=15 the range is from 1.2 to 1.3 μΩ. The data from these two turns are representative of the range of behaviors observed throughout the magnet section. As can be seen from Figure 6 the adjacent strand resistance is typically at least an order of magnitude less than the crossover resistance and these values themselves can vary over an order of magnitude. The spread in the data at a given point along the x-axis can exceed the measurement error, indicating that individual resistances within the crossover and adjacent strand networks are not identical.

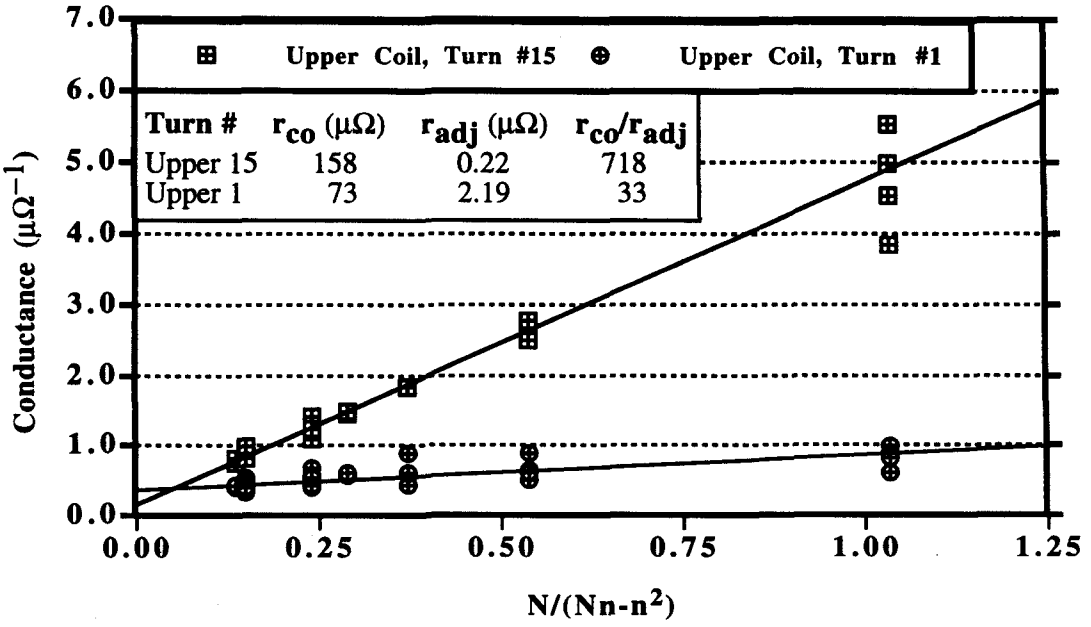

Figure 6. Measured Interstrand Conductance as a Function of the Strand Separation Parameter $N/(Nn-n^2)$ for Two Different Turns of the Upper Coil. The straight lines are linear fits to the data and the values reported for r_{co} and r_{adj} are taken from these linear fits.

Figure 7 shows the interstrand average resistance distribution through both the upper and the lower coils. There is a tendency for the interstrand resistance to go down in the direction towards the midplane. This is more pronounced for the upper coil than for the lower coil. Away from the pole turns the average interstrand resistance values for the upper and lower coils are about the same.. The fine structure of the interstrand resistance distribution shows variation of the average value from turn to turn which is greater than the measurement error. In this respect it is interesting to note that all wedge turns on the pole side have somewhat lower interstrand resistance than the wedge turns from the midplane side. Also, one can see that for some unknown reason turn #6 (upper coil) has unusually high interstrand resistance. Finally, the experimental data for the average interstrand resistance of DSA328 inner coil presented in this work does not confirm the

interstrand resistance distribution evaluated from multipoles decay measurements.[2] The expected interstrand resistance distribution from analysis of multipoles decay measurements would be relatively large interstrand resistance at the pole and midplane and a minimum in the multiturn section of the coil. There has been speculation that interstrand resistance distribution closely follows stress distribution in dipole magnets. This data does not simply correlate with stress distribution calculations performed for SSC dipole magnets.[3]

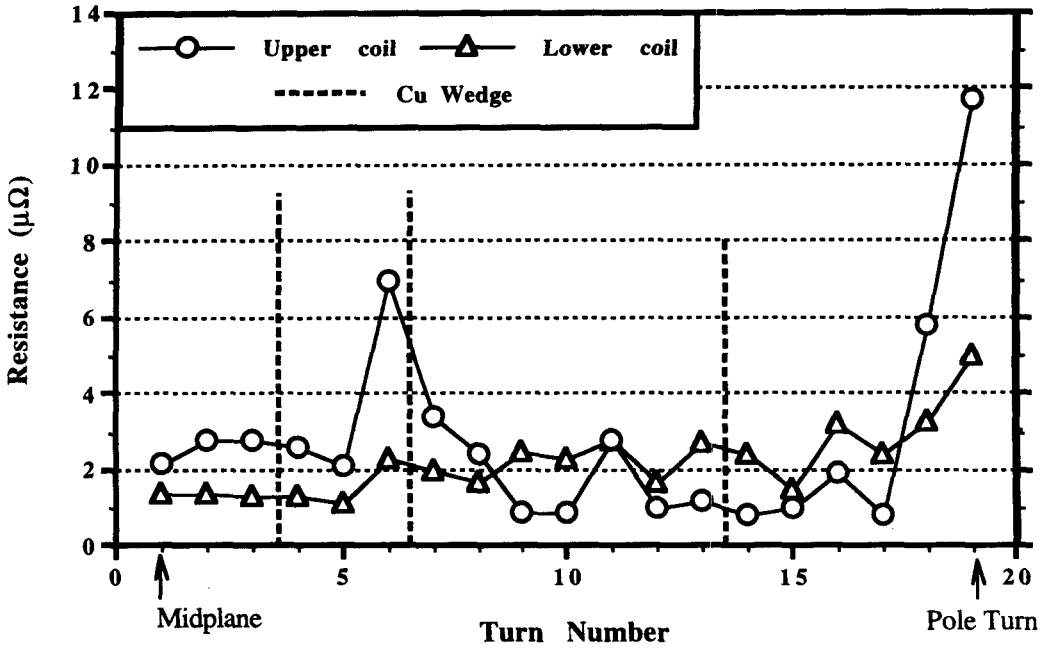

Figure 7. Distribution of Average Nonadjacent Interstrand Resistance as a Function of Turn Number for the Upper and Lower Coils. The locations of copper spacing wedges, as sketched in Figure 3, are indicated by dotted lines.

The average interstrand resistance of adjacent strands obtained for DSA328 upper and lower coils (see Appendix I, pole turn through turn #15) follows the same distribution tendency. The average interstrand resistance decreases in the direction of the midplane.

4.0 CONCLUSION

The first model for evaluating the interstrand resistance in cables for superconducting accelerator magnets has been proposed by G. Morgan [4]. Morgan's model assumes interstrand resistance between any two strands of the cable to be identical. This model was developed for braid cables but it has also been used for evaluation of AC loss in Rutherford type cables.

The present work shows that the interstrand resistances in a keystoned Rutherford cable under standard magnet prestress are not identical. Resistance between adjacent strands is considerably lower than the non-adjacent strand resistance. Also, resistances between the adjacent strands themselves as well as between non-adjacent strands vary and in many cases are far from identical. In a magnet coil under pressure the Rutherford cable is a very compact structure and can probably be considered as a specific network of superconducting wires located in a "solid" copper matrix with two or three-dimensional anisotropy of electrical resistivity. The anisotropy of electrical resistivity must account for different contact resistances in a direction perpendicular to the wide face of the cable (crossover contact) and along the axis of the strands or the cable (cable edge rollover and strand side by side contacts). Such a physical model will be qualitatively

similar to the anisotropic continuum model first proposed by J. Carr for describing electromagnetic coupling in multifilamentary superconductors.[5]

The simple model presented in this work suggests that crossover contacts between nonadjacent strands in this magnet are much more resistive than adjacent strand contacts.

The present work shows that the average nonadjacent interstrand resistance as well as the average adjacent interstrand resistance in DSA328 decreases from the pole turn to the midplane turn. Also, the average values for the pole turn interstrand resistance of the upper and lower coils are different. Because the cable used for both DSA328 inner coils is identical (batch # 7, SSC-3-S-00025 and SSC-3-S-00026) the difference in interstrand resistance must come from some differences in coil technology (curing) and/or magnet assembly (coil dimensions, prestress, *etc.*).

In situ interstrand studies of DCA312 sections which are already in progress will verify if the findings in the DSA328 section have only local or a more general bases in terms of interstrand resistance distribution, upper-lower coil interstrand resistance difference, *etc.*

ACKNOWLEDGMENTS

The others wish to thank T. Jarrett for helping with sample preparations, and T. Jaffery for providing DSA328 quench sensitivity and AC loss data.

REFERENCES

1. M. Wake, Ramp rate behavior of SSC magnets, MSD Technical Note # MD-MKA-0-93-007, SSCL, June 23, 1993.
2. T. Ogitsu *et. al.*, Influence of eddy currents on magnetic field harmonics, Proc. ICFA Workshop on AC Superconductivity, 23, KEK, Tsukuba, Japan, 1992
3. J. Turner, Mechanical Analysis of the W6733H Cross-Section, MSD Technical Note #MD-TA-143, SSCL, July 1990.
4. G. H. Morgan, Eddy currents in flat metal-filled superconducting braids, J. Appl. Phys., **44**, 3319 (1973)
5. W. J. Carr, Jr. , AC Loss and macroscopic theory of superconductors, Gordon & Breach, N.Y., 1983

APPENDIX I

UPPER COIL		LOWER COIL	
Strand #	Resistance (μΩ)	Strand #	Resistance (μΩ)
Turn #19		(Pole Turn)	
(1)-(6)	10.4	(1)-(6)	5.3
(1)-(11)	14.1	(1)-(11)	6
(1)-(16)	19.6	(1)-(16)	4.6
(1)-(21)	16.5	(1)-(21)	5.6
(1)-(26)	11.8	(1)-(26)	5.2
(6)-(11)	12.2	(6)-(11)	5.3
(6)-(16)	18.1	(6)-(16)	5.3
(6)-(21)	14.9	(6)-(21)	5.6
(6)-(26)	10.9	(6)-(26)	5.1
(11)-(16)	7.5	(11)-(16)	5.5
(11)-(21)	4.2	(11)-(21)	5.1
(11)-(26)	6.5	(11)-(26)	4.4
(16)-(21)	7.2	(16)-(21)	4.9
(16)-(26)	12.5	(16)-(26)	4.9
(21)-(26)	8.8	(21)-(26)	3.2
(1)-(2)	2.2	(1)-(2)	1.8
(1)-(3)	3.3	(1)-(3)	5.3
(1)-(4)	9.4	(1)-(4)	5.5
(1)-(5)	10.4	(1)-(5)	4.7
(1)-(6)	10.9	(1)-(6)	5.3
(2)-(3)	1.2	(2)-(3)	4.5
(2)-(4)	8.2	(2)-(4)	5.2
(2)-(5)	9.5	(2)-(5)	4.7
(2)-(6)	10.1	(2)-(6)	4.6
(3)-(4)	7.6	(3)-(4)	3.2
(3)-(5)	8.9	(3)-(5)	4.8
(3)-(6)	9.6	(3)-(6)	5.6
(4)-(5)	2.3	(4)-(5)	3.1
(4)-(6)	3.6	(4)-(6)	4.7
(5)-(6)	1.5	(5)-(6)	2.5
Turn # 18			
(1)-(6)	4.2	(1)-(6)	3.7
(1)-(11)	5.8	(1)-(11)	3.2
(1)-(16)	5.2	(1)-(16)	3.5
(1)-(21)	6.3	(1)-(21)	4.1
(1)-(26)	4.7	(1)-(26)	3.4
(6)-(11)	3.8	(6)-(11)	2.8
(6)-(16)	5.6	(6)-(16)	3.7
(6)-(21)	7.5	(6)-(21)	4.5
(6)-(26)	7.7	(6)-(26)	3.9
(11)-(16)	4.5	(11)-(16)	2.3
(11)-(21)	6.9	(11)-(21)	3.4
(11)-(26)	7.8	(11)-(26)	2.9
(16)-(21)	4.3	(16)-(21)	2.9
(16)-(26)	6.5	(16)-(26)	2.9
(21)-(26)	6.5	(21)-(26)	2.8

UPPER COIL		LOWER COIL	
Strand #	Resistance (μΩ)	Strand #	Resistance (μΩ)
Turn #18			
(1)-(2)	0.8	(1)-(2)	1.6
(1)-(3)	1.9	(1)-(3)	2.4
(1)-(4)	3.7	(1)-(4)	3
(1)-(5)	4.5	(1)-(5)	3.5
(1)-(6)	5	(1)-(6)	3.7
(2)-(3)	1.2	(2)-(3)	1.2
(2)-(4)	3.2	(2)-(4)	2.2
(2)-(5)	4.1	(2)-(5)	2.7
(2)-(6)	4.6	(2)-(6)	3.2
(3)-(4)	2.4	(3)-(4)	1.3
(3)-(5)	3.3	(3)-(5)	2
(3)-(6)	4	(3)-(6)	3.2
(4)-(5)	1.4	(4)-(5)	1
(4)-(6)	2.3	(4)-(6)	2
(5)-(6)	1.2	(5)-(6)	1.3
Turn #17			
(1)-(6)	0.6	(1)-(6)	2.7
(1)-(11)	0.9	(1)-(11)	2.5
(1)-(16)	1	(1)-(16)	2.4
(1)-(21)	0.8	(1)-(21)	2.5
(1)-(26)	0.6	(1)-(26)	1.9
(6)-(11)		(6)-(11)	2
(6)-(16)	0.5	(6)-(16)	2.5
(6)-(21)	1	(6)-(21)	2.9
(6)-(26)	1	(6)-(26)	2.8
(11)-(16)		(11)-(16)	1.8
(11)-(21)		(11)-(21)	2.5
(11)-(26)		(11)-(26)	2.5
(16)-(21)	0.6	(16)-(21)	2.1
(16)-(26)	0.9	(16)-(26)	2.3
(21)-(26)	0.6	(21)-(26)	2
(1)-(2)	0.14	(1)-(2)	0.8
(1)-(3)	0.28	(1)-(3)	1.8
(1)-(4)	0.46	(1)-(4)	2.2
(1)-(5)	0.56	(1)-(5)	2.4
(1)-(6)	0.12	(1)-(6)	2.8
(2)-(3)	0.3	(2)-(3)	1.2
(2)-(4)	0.42	(2)-(4)	2.1
(2)-(5)	0.54	(2)-(5)	2.3
(2)-(6)	0.18	(2)-(6)	2.8
(3)-(4)	0.32	(3)-(4)	1.4
(3)-(5)	0.44	(3)-(5)	1.8
(3)-(6)	0.14	(3)-(6)	2.5
(4)-(5)	0.3	(4)-(5)	0.7
(4)-(6)	0.16	(4)-(6)	1.9
(5)-(6)	1.2	(5)-(6)	1.4

UPPER COIL		LOWER COIL	
Strand #	Resistance (μΩ)	Strand #	Resistance (μΩ)
Turn #16			
(1)-(6)	1.3	(1)-(6)	4.2
(1)-(11)	2.5	(1)-(11)	3.6
(1)-(16)	2.6	(1)-(16)	2.8
(1)-(21)	2.1	(1)-(21)	3.3
(1)-(26)	1.2	(1)-(26)	2.5
(6)-(11)	1.7	(6)-(11)	3.4
(6)-(16)	2.3	(6)-(16)	3.9
(6)-(21)	2.3	(6)-(21)	4.3
(6)-(26)	2	(6)-(26)	4.2
(11)-(16)	1.5	(11)-(16)	3.2
(11)-(21)	1.9	(11)-(21)	3
(11)-(26)	2.4	(11)-(26)	3.1
(16)-(21)	1.3	(16)-(21)	2
(16)-(26)	1.6	(16)-(26)	2.4
(21)-(26)	1.4	(21)-(26)	2.1
(1)-(2)	0.3	(1)-(2)	1.6
(1)-(3)	0.6	(1)-(3)	2.6
(1)-(4)	0.8	(1)-(4)	3.1
(1)-(5)	1.2	(1)-(5)	3.9
(1)-(6)	1.3	(1)-(6)	4.2
(2)-(3)	0.35	(2)-(3)	1.5
(2)-(4)	0.6	(2)-(4)	2.4
(2)-(5)	0.85	(2)-(5)	3.5
(2)-(6)	1.2	(2)-(6)	4.1
(3)-(4)	0.25	(3)-(4)	1.3
(3)-(5)	0.6	(3)-(5)	2.8
(3)-(6)	0.9	(3)-(6)	3.8
(4)-(5)	0.4	(4)-(5)	2.1
(4)-(6)	0.7	(4)-(6)	3.3
(5)-(6)	0.4	(5)-(6)	2.4
Turn #15			
(1)-(6)	0.8	(1)-(6)	1.3
(1)-(11)	1.2	(1)-(11)	1.9
(1)-(16)	1.2	(1)-(16)	1.8
(1)-(21)	1.1	(1)-(21)	1.5
(1)-(26)	0.7	(1)-(26)	1
(6)-(11)	0.8	(6)-(11)	1.7
(6)-(16)	1.2	(6)-(16)	2
(6)-(21)	1.3	(6)-(21)	1.9
(6)-(26)	1.2	(6)-(26)	1.8
(11)-(16)	0.9	(11)-(16)	1.1
(11)-(21)	1.2	(11)-(21)	1.6
(11)-(26)	1.2	(11)-(26)	1.8
(16)-(21)	0.8	(16)-(21)	1.1
(16)-(26)	1	(16)-(26)	1.6
(21)-(26)	0.7	(21)-(26)	1

UPPER COIL		LOWER COIL	
Strand #	Resistance (μΩ)	Strand #	Resistance (μΩ)
Turn #15			
(1)-(2)	0.22	(1)-(2)	0.2
(1)-(3)	0.36	(1)-(3)	0.48
(1)-(4)	0.54	(1)-(4)	0.82
(1)-(5)	0.68	(1)-(5)	1.1
(1)-(6)	0.8	(1)-(6)	1.4
(2)-(3)	0.18	(2)-(3)	0.3
(2)-(4)	0.38	(2)-(4)	0.68
(2)-(5)	0.54	(2)-(5)	0.92
(2)-(6)	0.66	(2)-(6)	1.3
(3)-(4)	0.26	(3)-(4)	0.4
(3)-(5)	0.4	(3)-(5)	0.68
(3)-(6)	0.54	(3)-(6)	1.1
(4)-(5)	0.18	(4)-(5)	0.32
(4)-(6)	0.36	(4)-(6)	0.78
(5)-(6)	0.2	(5)-(6)	0.52
Turn #14			
(1)-(6)	0.6	(1)-(6)	2.7
(1)-(11)	0.85	(1)-(11)	3.3
(1)-(16)	0.85	(1)-(16)	2.7
(1)-(21)	0.9	(1)-(21)	2.7
(1)-(26)	0.6	(1)-(26)	1.9
(6)-(11)	0.6	(6)-(11)	2.3
(6)-(16)	0.85	(6)-(16)	2.9
(6)-(21)	1	(6)-(21)	3
(6)-(26)	0.95	(6)-(26)	3.1
(11)-(16)	0.65	(11)-(16)	2.1
(11)-(21)	0.95	(11)-(21)	2.6
(11)-(26)	1.05	(11)-(26)	3
(16)-(21)	0.6	(16)-(21)	1.2
(16)-(26)	0.9	(16)-(26)	2
(21)-(26)	0.7	(21)-(26)	1.2
Turn #13			
(1)-(6)	1	(1)-(6)	2.9
(1)-(11)	1.6	(1)-(11)	3.6
(1)-(16)	1	(1)-(16)	2.9
(1)-(21)	1	(1)-(21)	2.6
(1)-(26)	0.85	(1)-(26)	2.3
(6)-(11)	1.4	(6)-(11)	2.5
(6)-(16)	1.4	(6)-(16)	2.5
(6)-(21)	1.4	(6)-(21)	2.8
(6)-(26)	1.5	(6)-(26)	3.2
(11)-(16)	1.2	(11)-(16)	2.3
(11)-(21)	1.15	(11)-(21)	2.8
(11)-(26)	1.75	(11)-(26)	3.4
(16)-(21)	1.15	(16)-(21)	1.8
(16)-(26)	0.7	(16)-(26)	2.6
(21)-(26)	0.7	(21)-(26)	1.9

UPPER COIL		LOWER COIL	
Strand #	Resistance (μΩ)	Strand #	Resistance (μΩ)
Turn #12			
(1)-(6)	0.65	(1)-(6)	1.9
(1)-(11)	1.05	(1)-(11)	2.3
(1)-(16)	1.25	(1)-(16)	2.1
(1)-(21)	1.1	(1)-(21)	1.9
(1)-(26)	0.65	(1)-(26)	1.4
(6)-(11)	0.65	(6)-(11)	1.6
(6)-(16)	1.15	(6)-(16)	2.1
(6)-(21)	1.25	(6)-(21)	2.3
(6)-(26)	1.1	(6)-(26)	2.1
(11)-(16)	0.9	(11)-(16)	1.5
(11)-(21)	1.3	(11)-(21)	1.9
(11)-(26)	1.3	(11)-(26)	1.1
(16)-(21)	0.95	(16)-(21)	1.3
(16)-(26)	1.25	(16)-(26)	1.6
(21)-(26)	0.8	(21)-(26)	1
Turn #11			
(1)-(6)	1.8	(1)-(6)	2.4
(1)-(11)	3.1	(1)-(11)	3.1
(1)-(16)	3.4	(1)-(16)	3.4
(1)-(21)	3	(1)-(21)	2.6
(1)-(26)	1.7	(1)-(26)	1.6
(6)-(11)	2.2	(6)-(11)	2.2
(6)-(16)	3.3	(6)-(16)	3.5
(6)-(21)	3.4	(6)-(21)	3.3
(6)-(26)	2.8	(6)-(26)	3
(11)-(16)	2.8	(11)-(16)	2.8
(11)-(21)	3.6	(11)-(21)	3.3
(11)-(26)	3.5	(11)-(26)	3.4
(16)-(21)	2.5	(16)-(21)	2.6
(16)-(26)	3.1	(16)-(26)	3.1
(21)-(26)	2.1	(21)-(26)	1.7
Turn #10			
(1)-(6)	0.6	(1)-(6)	2
(1)-(11)	1.05	(1)-(11)	2.7
(1)-(16)	1.15	(1)-(16)	2.8
(1)-(21)	0.95	(1)-(21)	2.5
(1)-(26)	0.55	(1)-(26)	1.6
(6)-(11)	0.75	(6)-(11)	1.8
(6)-(16)	1.05	(6)-(16)	2.8
(6)-(21)	1.1	(6)-(21)	2.9
(6)-(26)	0.9	(6)-(26)	2.4
(11)-(16)	0.8	(11)-(16)	2.2
(11)-(21)	1.15	(11)-(21)	2.7
(11)-(26)	1.1	(11)-(26)	2.7
(16)-(21)	0.8	(16)-(21)	1.9
(16)-(26)	0.95	(16)-(26)	2.4
(21)-(26)	0.6	(21)-(26)	1.5

UPPER COIL		LOWER COIL	
Strand #	Resistance (μΩ)	Strand #	Resistance (μΩ)
Turn #9			
(1)-(6)	0.6	(1)-(6)	1.9
(1)-(11)	0.9	(1)-(11)	2.8
(1)-(16)	1.1	(1)-(16)	2.9
(1)-(21)	1	(1)-(21)	2.5
(1)-(26)	0.6	(1)-(26)	
(6)-(11)	0.6	(6)-(11)	2.3
(6)-(16)	1.05	(6)-(16)	2.9
(6)-(21)	1.1	(6)-(21)	2.9
(6)-(26)	0.9	(6)-(26)	
(11)-(16)	0.85	(11)-(16)	2
(11)-(21)	1.05	(11)-(21)	2.8
(11)-(26)	1.05	(11)-(26)	
(16)-(21)	0.7	(16)-(21)	2.3
(16)-(26)	1	(16)-(26)	
(21)-(26)	0.65	(21)-(26)	
Turn #8			
(1)-(6)	1.8	(1)-(6)	1.1
(1)-(11)	2.6	(1)-(11)	2.1
(1)-(16)	2.4	(1)-(16)	2.2
(1)-(21)	2.4	(1)-(21)	1.6
(1)-(26)	1.6	(1)-(26)	1
(6)-(11)	2.2	(6)-(11)	1.5
(6)-(16)	2.7	(6)-(16)	2
(6)-(21)	2.9	(6)-(21)	1.7
(6)-(26)	2.6	(6)-(26)	1.4
(11)-(16)	2.4	(11)-(16)	1.8
(11)-(21)	2.9	(11)-(21)	2.1
(11)-(26)	2.8	(11)-(26)	2.2
(16)-(21)	2	(16)-(21)	1.4
(16)-(26)	2.3	(16)-(26)	2.1
(21)-(26)	1.8	(21)-(26)	1.2
Turn #7			
(1)-(6)	3.7	(1)-(6)	1.1
(1)-(11)	3.8	(1)-(11)	2.3
(1)-(16)	3.4	(1)-(16)	2.3
(1)-(21)	3.5	(1)-(21)	1.7
(1)-(26)	2.4	(1)-(26)	1.3
(6)-(11)	3.5	(6)-(11)	1.9
(6)-(16)	3.7	(6)-(16)	2.1
(6)-(21)	4.2	(6)-(21)	2
(6)-(26)	3.7	(6)-(26)	2
(11)-(16)	3.2	(11)-(16)	1.8
(11)-(21)	3.9	(11)-(21)	2.6
(11)-(26)	3.4	(11)-(26)	2.9
(16)-(21)	3.3	(16)-(21)	2
(16)-(26)	3	(16)-(26)	2.6
(21)-(26)	2.7	(21)-(26)	1.8

UPPER COIL		LOWER COIL	
Strand #	Resistance (μΩ)	Strand #	Resistance (μΩ)
Turn #6			
(1)-(6)	7.5	(1)-(6)	1.1
(1)-(11)	8.2	(1)-(11)	2.5
(1)-(16)	6.9	(1)-(16)	2.4
(1)-(21)	6.3	(1)-(21)	2.3
(1)-(26)	4.8	(1)-(26)	1.4
(6)-(11)	9	(6)-(11)	2.1
(6)-(16)	8.2	(6)-(16)	2.3
(6)-(21)	7.8	(6)-(21)	2.4
(6)-(26)	6.6	(6)-(26)	2.1
(11)-(16)	8.5	(11)-(16)	2.1
(11)-(21)	8	(11)-(21)	2.8
(11)-(26)	6.5	(11)-(26)	3
(16)-(21)	6.8	(16)-(21)	2.1
(16)-(26)	5.5	(16)-(26)	2.9
(21)-(26)	4.6	(21)-(26)	2.3
Turn #5			
(1)-(6)	1.7	(1)-(6)	0.65
(1)-(11)	2.7	(1)-(11)	1.15
(1)-(16)	2.4	(1)-(16)	1.4
(1)-(21)	1.8	(1)-(21)	1.3
(1)-(26)	1.3	(1)-(26)	0.8
(6)-(11)	2.4	(6)-(11)	0.8
(6)-(16)	2.4	(6)-(16)	1.3
(6)-(21)	2.1	(6)-(21)	1.45
(6)-(26)	1.8	(6)-(26)	1.15
(11)-(16)	2.6	(11)-(16)	1
(11)-(21)	2.5	(11)-(21)	1.45
(11)-(26)	2.5	(11)-(26)	1.4
(16)-(21)	1.9	(16)-(21)	0.95
(16)-(26)	2.2	(16)-(26)	12.35
(21)-(26)	1.4	(21)-(26)	0.9
Turn #4			
(1)-(6)	2	(1)-(6)	0.7
(1)-(11)	3.1	(1)-(11)	1.4
(1)-(16)	2.7	(1)-(16)	1.6
(1)-(21)	2.3	(1)-(21)	1.35
(1)-(26)	1.9	(1)-(26)	0.8
(6)-(11)	2.7	(6)-(11)	0.9
(6)-(16)	2.8	(6)-(16)	1.5
(6)-(21)	2.8	(6)-(21)	1.5
(6)-(26)	2.7	(6)-(26)	1.25
(11)-(16)	2.8	(11)-(16)	1.15
(11)-(21)	3.1	(11)-(21)	1.65
(11)-(26)	3.2	(11)-(26)	1.6
(16)-(21)	2.4	(16)-(21)	1.15
(16)-(26)	2.6	(16)-(26)	1.55
(21)-(26)	1.5	(21)-(26)	0.95

UPPER COIL		LOWER COIL	
Strand #	Resistance (μΩ)	Strand #	Resistance (μΩ)
Turn #3			
(1)-(6)	2.5	(1)-(6)	0.7
(1)-(11)	3.1	(1)-(11)	1.4
(1)-(16)	2.8	(1)-(16)	1.7
(1)-(21)	2.9	(1)-(21)	1.5
(1)-(26)	2	(1)-(26)	1
(6)-(11)	2.4	(6)-(11)	1
(6)-(16)	3	(6)-(16)	1.6
(6)-(21)	3.2	(6)-(21)	1.7
(6)-(26)	3	(6)-(26)	1.4
(11)-(16)	2.8	(11)-(16)	1.1
(11)-(21)	3.2	(11)-(21)	1.6
(11)-(26)	3.1	(11)-(26)	1.7
(16)-(21)	2.5	(16)-(21)	1.1
(16)-(26)	2.7	(16)-(26)	1.6
(21)-(26)	2.2	(21)-(26)	1
Turn #2			
(1)-(6)	2.6	(1)-(6)	0.9
(1)-(11)	2.75	(1)-(11)	1.5
(1)-(16)	3.2	(1)-(16)	1.7
(1)-(21)	2.6	(1)-(21)	1.5
(1)-(26)	1.9	(1)-(26)	1
(6)-(11)	2.7	(6)-(11)	1.1
(6)-(16)	3.2	(6)-(16)	1.6
(6)-(21)	3.2	(6)-(21)	1.7
(6)-(26)	2	(6)-(26)	1.4
(11)-(16)	2.9	(11)-(16)	1.3
(11)-(21)	3.2	(11)-(21)	1.7
(11)-(26)	2.5	(11)-(26)	1.8
(16)-(21)	3.6	(16)-(21)	1.2
(16)-(26)	2.8	(16)-(26)	1.7
(21)-(26)	2.3	(21)-(26)	1.1
Turn #1 (Midplane)			
(1)-(6)	2.3	(1)-(6)	0.95
(1)-(11)	2.3	(1)-(11)	1.45
(1)-(16)	2.4	(1)-(16)	1.5
(1)-(21)	1.8	(1)-(21)	1.45
(1)-(26)	1.7	(1)-(26)	1.3
(6)-(11)	2.3	(6)-(11)	1.15
(6)-(16)	2.8	(6)-(16)	1.45
(6)-(21)	2.4	(6)-(21)	1.6
(6)-(26)	2.5	(6)-(26)	1.6
(11)-(16)	2.3	(11)-(16)	1.35
(11)-(21)	2	(11)-(21)	1.9
(11)-(26)	2.2	(11)-(26)	1.9
(16)-(21)	2.1	(16)-(21)	1.3
(16)-(26)	2.3	(16)-(26)	1.4
(21)-(26)	1.4	(21)-(26)	1.35

UPPER COIL		LOWER COIL	
Strand #	Resistance ($\mu\Omega$)	Strand #	Resistance ($\mu\Omega$)
Turn #1 (Midplane)			
(1)-(2)	1	(3)-(9)	1.05
(1)-(3)	1.5	(3)-(14)	1.4
(1)-(4)	2.1	(3)-(19)	1.15
(1)-(5)	1.7	(3)-(24)	1.6
(1)-(6)	1.8	(3)-(29)	1
(2)-(3)	1	(9)-(14)	1.1
(2)-(4)	1.9	(9)-(19)	1.35
(2)-(5)	1.6	(9)-(24)	1.95
(2)-(6)	1.6	(9)-(29)	1.45
(3)-(4)	1.6	(14)-(19)	1.4
(3)-(5)	1.6	(14)-(24)	2
(3)-(6)	1.1	(14)-(29)	1.55
(4)-(5)	1.1	(19)-(24)	1.55
(4)-(6)	1.1	(19)-(29)	1.1
(5)-(6)	1.2	(24)-(29)	1.3

APPENDIX II

Contact between strands in a multistrand superconducting cable occurs in two ways; between adjacent strands both axially and at the 'rollover' points and between nonadjacent strands at their crossover points. The adjacent strand rollover contact is different from nonadjacent strand crossover contact because rollover occurs at the cable edges where the strands are moving from the top to the bottom of the cable or vice versa. This results in increased deformation of the strands at the rollover as well as a larger contact area. In this analysis it is not necessary to distinguish between axial and rollover contact between adjacent strands and so adjacent strands will be referred to simply as having 'adjacent contact'. The current path between any two strands in the cable can then be approximated as two parallel resistor networks, one made up of crossover contacts and the other of the adjacent contacts. The relevant formulae will be derived by neglecting first adjacent contacts and second by neglecting nonadjacent contacts.

Consider first the case where adjacent contacts are neglected for a cable made up of N strands exactly 1 pitch length long. Each strand pair makes 2 crossover contacts in this length. All contact resistances are assumed equal to r_{co}. The two contacts are in parallel so that the primary resistance is $r_{co}/2$. In addition to this primary resistance this model considers secondary resistances in which an intermediate strand participates. The secondary resistances are the sum of two primary resistances, r_{co}. This situation is illustrated in Figure A1 for a six strand cable. The paths between strands 1 and 3, for example, are 1-2-3, 1-3, 1-4-3, 1-5-3, 1-6-3, where 1-3 is the primary path and the rest are secondary. In general, there is one primary resistance and N-2 secondary resistances so that the net interstrand resistance is given by:

$$\frac{1}{R_{co}} = \frac{1}{r_{co}/2} + (N-2)\frac{1}{r_{co}} = \frac{N}{r_{co}} \tag{A1}$$

When cross over contacts are neglected the cable can be modeled as a circular path of series resistors, as shown in Figure A2. Current flow between any two strands will be along two paths, as illustrated. Assuming all adjacent resistances are equivalent, the total interstrand resistance in this case is given by:

$$\frac{1}{R_{adj}} = \frac{1}{nr_{adj}} + \frac{1}{(N-n)r_{adj}} = \frac{1}{r_{adj}}\frac{N}{(Nn-n^2)} \tag{A2}$$

where n is the distance in strand diameters between the strands of interest and N is the total number of strands. Equation A2 is a parabolic function of n having a maximum at n = N/2.

In reality the measured interstrand resistance will be the result of these two networks in parallel, or

$$\frac{1}{R_{tot}} = \frac{1}{R_{co}} + \frac{1}{R_{adj}} = \frac{N}{r_{co}} + \frac{1}{r_{adj}}\frac{N}{(Nn - n^2)} \tag{A3}$$

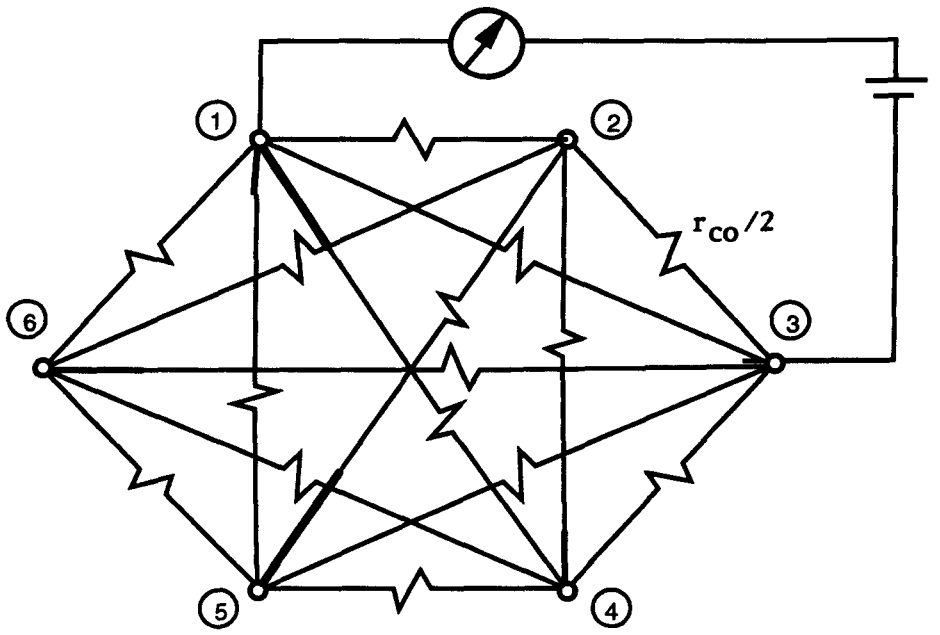

Figure A1. The Equivalent Circuit for Interstrand Resistance in a Six Strand Cable for the Case Where Adjacent Contact is Neglected.

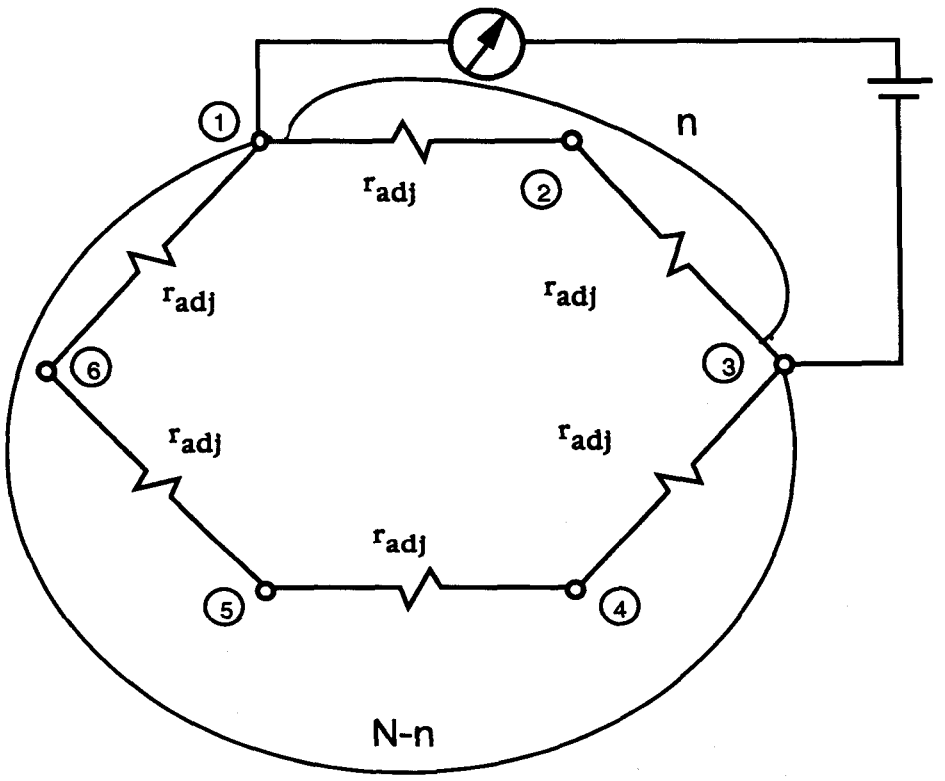

Figure A2. The Equivalent Circuit for Interstrand Resistance for the Case Where CrossOver Contact is Neglected.